

Stability of subnanometer MoS wires under realistic environment

Dominike A. P. de Deus,[†] Daniel F. Souza,[‡] Andréia L. da Rosa,[¶] Renato B. Pontes,[¶] and Th. Frauenheim^{*,||}

[†]*Instituto Federal de Educação, Ciência e Tecnologia de Goiás, Departamento de Áreas Acadêmicas, Campus Jataí, Ormindá Vieira de Freitas 775, 75804714 Jataí, Goiás, Brazil*

[‡]*Instituto Federal do Amazonas, 69020-120, Manaus, AM, Brazil*

[¶]*Instituto de Física, Universidade Federal de Goiás, Campus Samambaia, 74690-900, Goiânia, Goiás, Brazil*

[§]*Bremen Center for Computational Materials Science, University of Bremen, Am Fallturm 1, 28359, Bremen, Germany*

^{||}*Bremen Center for Computational Materials Science, University of Bremen, Am Fallturm 1, 28359 Bremen, Germany*

[⊥]*Shenzhen Computational Science and Applied Research Institute, Shenzhen, China*

[#]*Beijing Computational Science Research Center, Beijing, China*

E-mail: andreialuisa@ufg.br

Phone: +55 62 35211122

Abstract

We carried out first-principles density functional theory calculations of hydrogen and oxygen adsorption and diffusion on subnanometer MoS nanowires. The nanowires are robust against adsorption of hydrogen. On the other hand, interaction with oxygen

shows that the nanowires can oxidize with a small barrier. Our results open the path for understanding the behavior of MoS nanowires under realistic environment.

Introduction

The discovery of graphene has attracted the interest of the scientific community in other low-dimensional materials, such as transition-metal dichalcogenides (TMDCs), which exhibit novel physical and chemical properties with promising applications in nanotechnology.¹⁻³ In particular, single-layered MoS₂ possesses a sizeable electronic band gap of 1.8 eV, which may be useful for applications in high-end electronics, spintronics, optoelectronics, energy-harvesting, flexible electronics, and biomedicine.⁴⁻⁶

Recently transition metal chalcogenide (TMC) subnanometer nanowires have been fabricated by ion and electron beam techniques in MoS₂ layers.^{7,8} Contrary to single-layered MoS₂, MoS nanowires show metallic behavior.⁹ Such wires under tensile strain undergo a phase transformation is observed in the MoS NWs which results in tension-induced hardening in their tensile modulus.¹⁰ Furthermore, topological states in one-dimensional MoS nanowires have been proposed.¹¹

For several nanoscale applications, the interaction of nanostructures with the environment is very important, since it provides information on their stability against degradation. Usually two-dimensional MoS₂ exhibits unique surface effects but the interaction with hydrogen is limited by the amount of active sites.¹² Although hydrogen molecules diffuse on MoS₂ monolayers with a high energy barrier of 6.56 eV, their diffusion can be facilitated by applying strain which then reduces the diffusion barrier to 0.57 eV.¹³ Reactivity can further be improved via doping with transition metals.¹⁴ More recent results claim that oxygen strongly interacts with defective MoS₂ layers, enhancing their photoluminescence properties due to dissociation of O₂ on sulphur vacancies.¹⁵

Although the interaction of MoS₂ monolayers with oxygen and hydrogen has been largely

explored, investigations of MoS nanowires under realistic environments are still missing. In this paper we perform first-principles calculations density functional theory calculations of hydrogen and oxygen adsorption and diffusion on subnanometer MoS nanowires. We show that the nanowires have sizeable interaction with atomic hydrogen. However, dissociation of hydrogen molecules is hindered by a high energy barrier and unfavourable orientation of orbitals. On the other hand, oxidation of MoS wires may take place with a small diffusion barrier of oxygen atoms.

Computational details

The calculations are performed using density-functional theory (DFT),^{16,17} as implemented in the Vienna ab initio simulation package (VASP),¹⁸ The electron-ion interactions are taken into account using the Projector Augmented Wave (PAW) method. We employ the generalized gradient approximation (GGA-PBE)¹⁹ to describe the interaction between valence electrons. The Kohn-Sham orbitals are expanded in a plane wave basis set with an energy cutoff of 500 eV. The Brillouin Zone is sampled according to the Monkhorst-Pack method using a $(1 \times 1 \times 8)$ \mathbf{k} -points mesh. In order to determine the diffusion and reaction barriers we have performed CI-NEB^{20,21} calculations with seven images to search the minimum-energy reaction paths and saddle points between the initial state and final state configurations.

Results and discussion

Pristine nanowires

Mo and S atoms in pristine MoS nanowires are arranged by stacking of triangular layers rotated 180° along the nanowire axial direction, with three S atoms located at the vertices of the triangles and three Mo atoms located between the S atoms, as seen in Fig. 1. The calculated equilibrium lattice parameter along the axis wire is 4.39 Å. Contrary to single-

layered MoS_2 , pristine MoS nanowires show metallic behavior, as seen in Fig. 1(a). At Γ point the states with character d_{x^2} cross the Fermi level. Localized states with d_{z^2} character lie around 0.25 eV above the Fermi level, as seen in Fig. 1(b). In Fig. 1(c1) and (c2) (empty states) and (c3) and (c4) (occupied states) we show the orbital projected charge density in pristine wires. The empty states lie along the wire growth direction. We discuss the importance of orbital orientation later on.

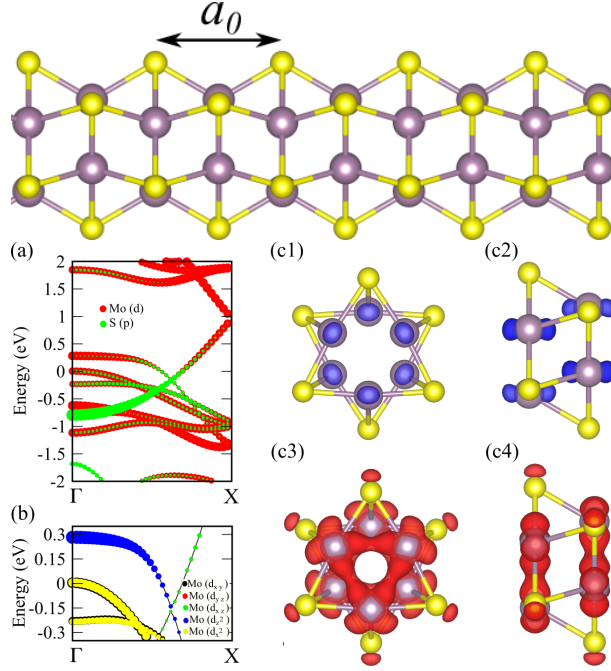


Figure 1: Relaxed geometry of an isolated MoS nanowire with lattice parameter a_0 along the wire growth direction. Electronic band structure of pristine MoS nanowire. a) Orbital decomposed band structure, b) Orbital Mo- d decomposed band structure and c1)-c4) band projected charge density. Blue are empty states (0.4 eV above the Fermi level) and red are occupied states (0.4 eV below the Fermi level, which is set at zero).

In order to understand the strength between MoS wires and hydrogen/oxygen we have calculated the adsorption energy according to:

$$E_{\text{ads}} = E_{\text{MoS-ad}} - E_{\text{MoS}} - \sum_i N_i \mu_i, \quad (1)$$

where $E_{\text{MoS-ad}}$ and E_{MoS} are the total energies of the MoS supercell with and without the adsorbate (hydrogen or oxygen). N_i and μ_i are the number and chemical potential of

hydrogen and oxygen in gas phase.

Table 1: Adsorption energy E_{ads} and diffusion/dissociation barrier ΔE of hydrogen and oxygen on MoS nanowires.

adsorbate	% (ML)	E_{ads} (eV)	ΔE (eV)
H on S	$1/12$	-0.55	
H on Mo	$1/12$	-0.30	
H on S	$1/24$	-0.80	
H on Mo	$1/24$	-0.60	
H ₂	$1/12$	-0.006	
H ₂	$1/24$	-0.005	
H	$1/24$		0.35
H ₂	$1/12$		2.60
H ₂	$1/24$		1.10
O on S	$1/12$	0.58	
O on Mo	$1/12$	-0.22	
O on S	$1/24$	-0.19	
O on Mo	$1/24$	-0.50	
O ₂	$1/12$	0.09	
O ₂	$1/24$	-0.25	
O	$1/24$		0.42
O ₂	$1/24$		0.20

We have considered adsorption of atomic and molecular hydrogen/oxygen. Concentrations of $1/12$ and $1/24$ monolayers (ML) which correspond to $(1 \times 1 \times 2)$ and $(1 \times 1 \times 1)$ unit cells, respectively, have been used. The results for the adsorption energy are shown in Table 1. For atomic hydrogen, coverages of $1/12$ ML shows that adsorption of atomic hydrogen atom has the lowest energy on a sulphur atom. This energy is higher by 0.25 eV than adsorption on a Mo atom. Smaller coverages of $1/24$ ML have a similar behavior. For hydrogen concentration of $1/24$ ML, S-H bond length is $d_{\text{S-H}} = 1.36 \text{ \AA}$. The relaxed structure is shown in Fig. 2(a). Atomic hydrogen prefers to be at ontop position, with the nanowire structure barely affected by the hydrogen atom. Charge density difference calculated according to $\Delta\rho = \rho_{\text{MoS-H}} - \rho_{\text{MoS}} - \rho_{\text{H}}$ is shown in Fig. 2(b) with the nanowire structure barely affected by the hydrogen atom. Total charge density with views along and perpendicular to the wire growth direction is shown in Fig. 2(c) and (d).

To corroborate with this picture we show the band structure of atomic hydrogen adsorbed

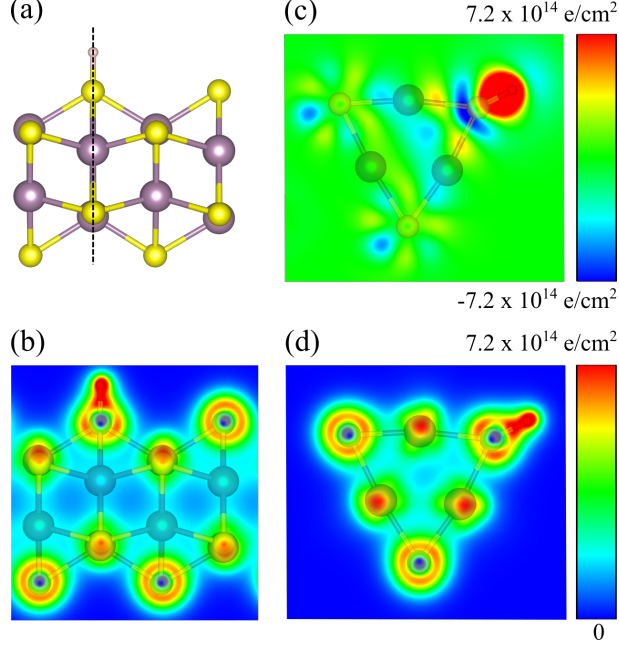


Figure 2: a) Relaxed structure of atomic hydrogen on MoS wires, b) charge difference ρ , c) total charge density (cut parallel) and d) cut perpendicular to the growth direction. Coverage of $1/24 \text{ ML}$.

on MoS nanowire for $1/24 \text{ ML}$ coverage. a) orbital projected band structure, b) PDOS on Mo-d, c) PDOS on S-p and d) PDOS on H-s in Fig.3.

In order to further understand this behavior we have calculated the corresponding orbital projected band structure. The states comes from Mo d_{z^2} (red) and d_{xz} (blue) and Mo d_{xy} (green) orbitals. Fig.4 reveals states with d_{z^2} character around the Fermi level which are shifted downwards in energy compared to the ones in pristine wires. The H-S bond has major contributions for the PDOS at -0.4 eV in Figs. 4(b)-(d).

Orbital projected charge density of atomic hydrogen on MoS nanowire at $1/24 \text{ ML}$ coverage. Close to the Fermi level we identified Mo- d_{xy} (a1) and (b1), Mo- d_{xz} (a2) and (b2) and Mo- d_{z^2} (a3) and (b3). In c) we show the projected band structure corresponding to these states.

The transition state along the considered path shown in Fig. 5 has the hydrogen adsorbed at the ontop position of a Mo atom. The dissociation barrier is 0.35 eV , as it can be seen in Fig.5 (j). By increasing the hydrogen coverage to $1/12 \text{ ML}$ the barrier is 2.60 eV (not shown).

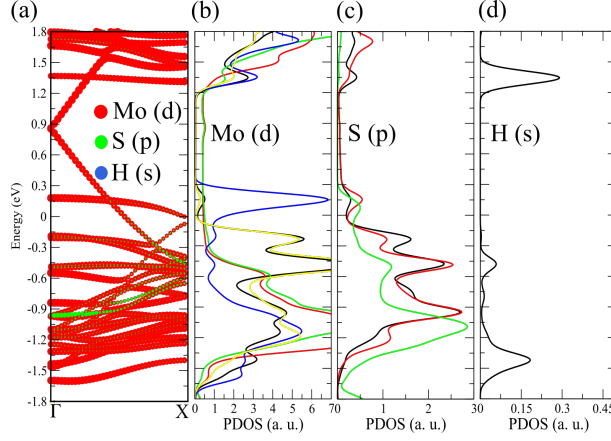


Figure 3: Band structure of atomic hydrogen adsorbed on MoS nanowire for $1/24$ ML coverage. a) orbital projected band structure, b) PDOS on Mo-d, c) PDOS on S-p and d) PDOS on H-s.

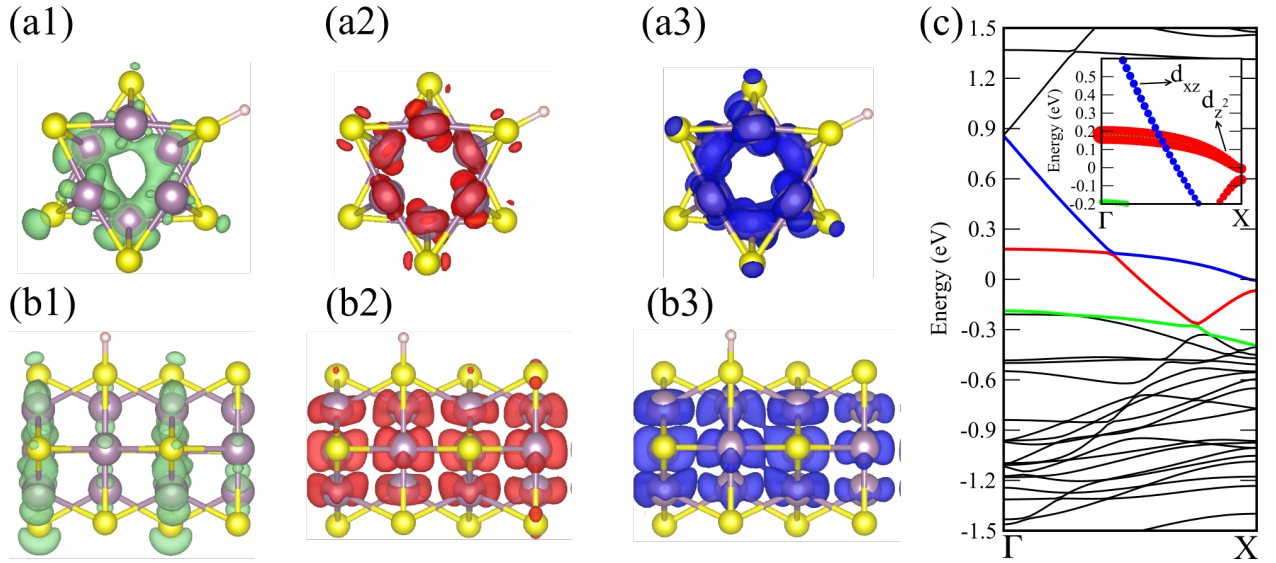


Figure 4: Orbital projected charge density of atomic hydrogen on MoS nanowire for $1/24$ ML coverage. a1) and b1) Mo- d_{xy} , a2) and b2) Mo- d_{xz} , a3) and b3) Mo- d_{z^2} and c) projected band structure corresponding to states shown in a) and b). The Fermi level is set at zero.

As a matter of comparison, usual barriers for atomic hydrogen are usually a few meV 0.05-0.3 eV, on hcp(0001), fcc(111) and bcc(110) metal surfaces,^{5,22} which is consistent with our results at low coverages.

Table 1 shows that contrary to atomic hydrogen, the adsorption energy of molecular hydrogen is only 6.00 meV. Furthermore, negligible difference is found for hydrogen concentrations of $1/24$ and $1/12$ ML. In order to further understand this behavior, we have calculated the dissociation barrier of hydrogen along the path shown in Fig. 5(a)-(i). Barrier of 1.10 eV.

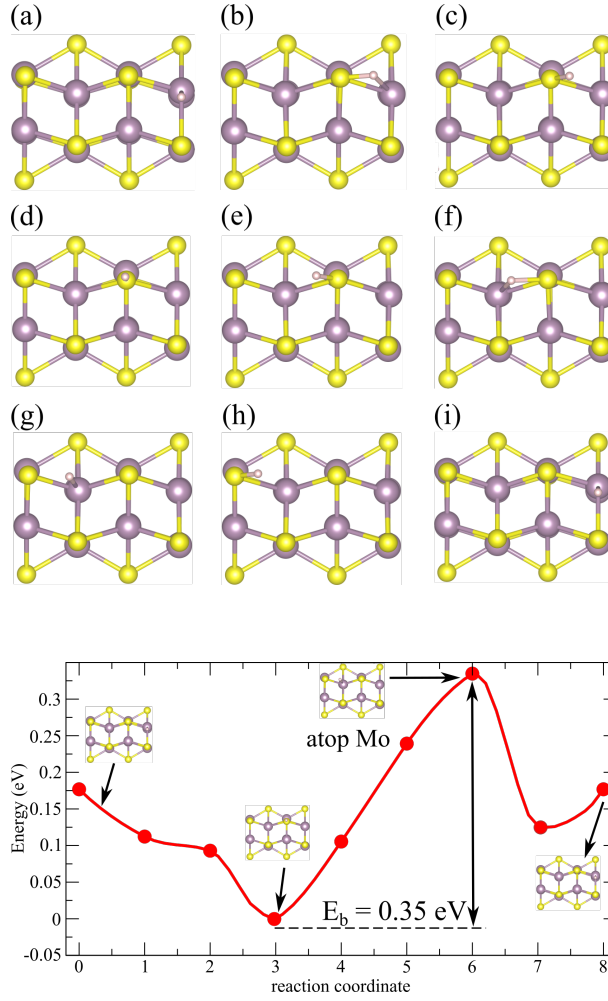


Figure 5: a)- i) Minimum-energy reaction path and j) diffusion barrier for atomic hydrogen on MoS nanowire for $1/24$ ML coverage.

The band structure of the most stable state in Fig. 6(a) is shown in Fig. 6(b).

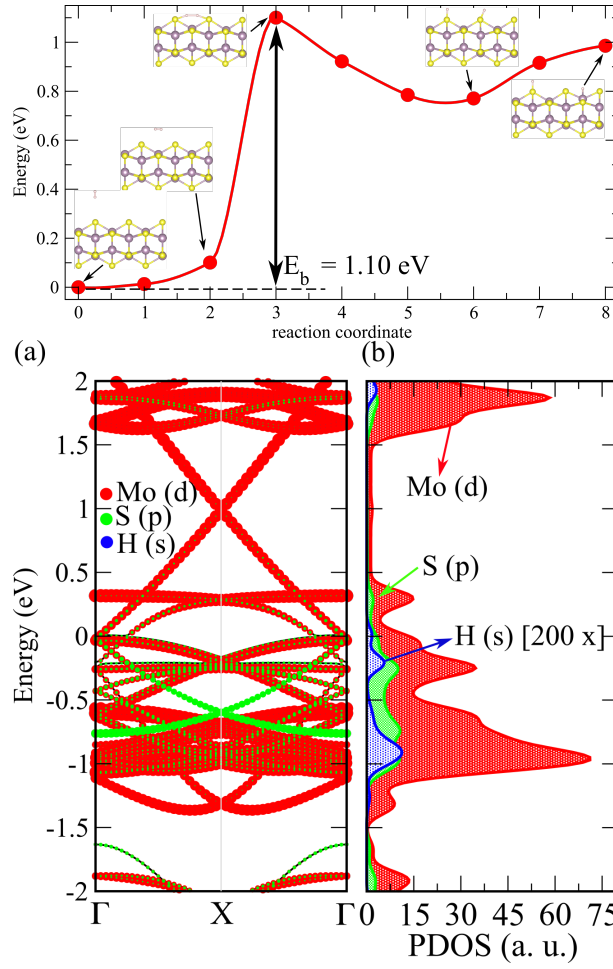


Figure 6: Dissociation barrier of a hydrogen molecule on MoS nanowire for $1/24$ ML coverage. Band structure and PDOS corresponding to the most stable state shown a).

Oxygen adsorption

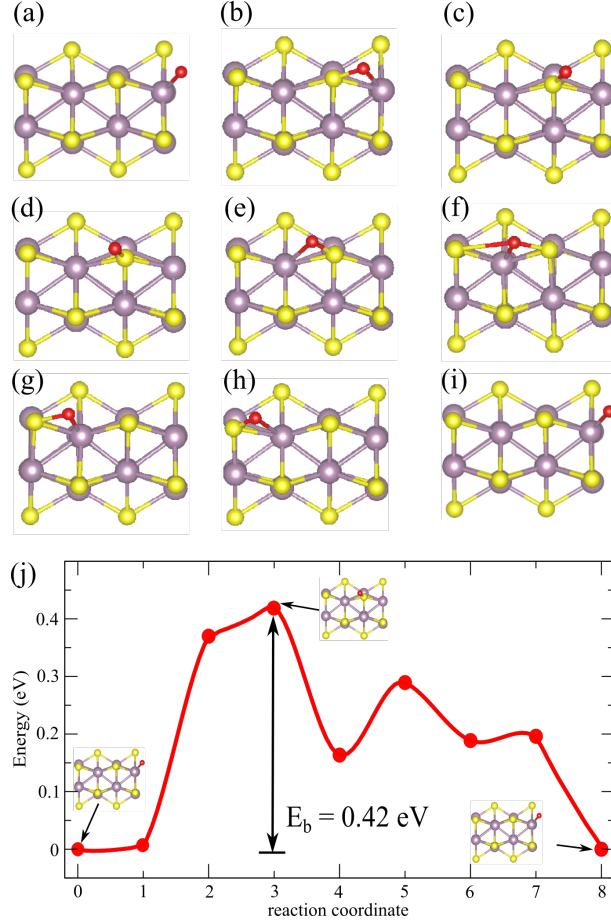


Figure 7: Minimum-energy reaction path for atomic oxygen atom on MoS nanowire with hydrogen adsorbed on Mo-S bridge for $1/24$ ML coverage.

Atomic oxygen atom adsorbs at a bridge position as shown in Fig.7(a). Starting from this configuration, Fig.7(a)-(i) show the minimum energy path with a diffusion barrier of 0.42 eV. The transition state corresponds to the oxygen atom close to an ontop position. The band structure corresponding to Fig.7(a)) is shown in Fig.8(j).

At $1/12$ ML oxygen concentration as shown in Fig.8 a) side view) and b) top view we have an endothermic reaction, as seen from Table 1. Interestingly enough, by decreasing the oxygen concentration to $1/24$ ML, the reaction turns out to be exothermic. The band structure is shown in Fig.10(c). The more stable structure for an oxygen molecule shows a small magnetic moment due to outwards relaxation of nearby Mo atoms. The presence

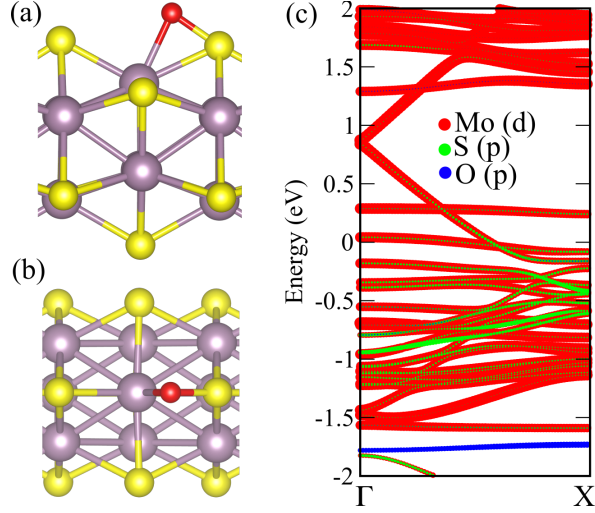


Figure 8: Band structure of atomic oxygen on MoS for the lowest energy structure shown in Fig. 7.

of the O_2 molecule near a Mo atom introduces $O-p_z$ states close to the Γ and X points. Furthermore, the valence band maximum (VBM) has mainly $Mo-d_{z^2}$ character, whereas the conduction band minimum (CBM) shows mixed $O-p_z$, $Mo-d_{xz}$ and $Mo-d_{yz}$ states, as seen in Fig. 10(d).

Conclusion

In this paper we perform first-principles calculations density functional theory calculations of hydrogen and oxygen adsorption and diffusion on subnanometer MoS nanowires. We show that the nanowires have sizeable interaction with atomic hydrogen, but little with hydrogen molecules. Furthermore, oxidation of MoS nanowires is feasible and occurs with a small barrier.

Acknowledgement

We acknowledge the financial support from the Brazilian Agency CNPq under grant number 313081/2017-4 and 305335/2020-0 and German Science Foundation (DFG) under the

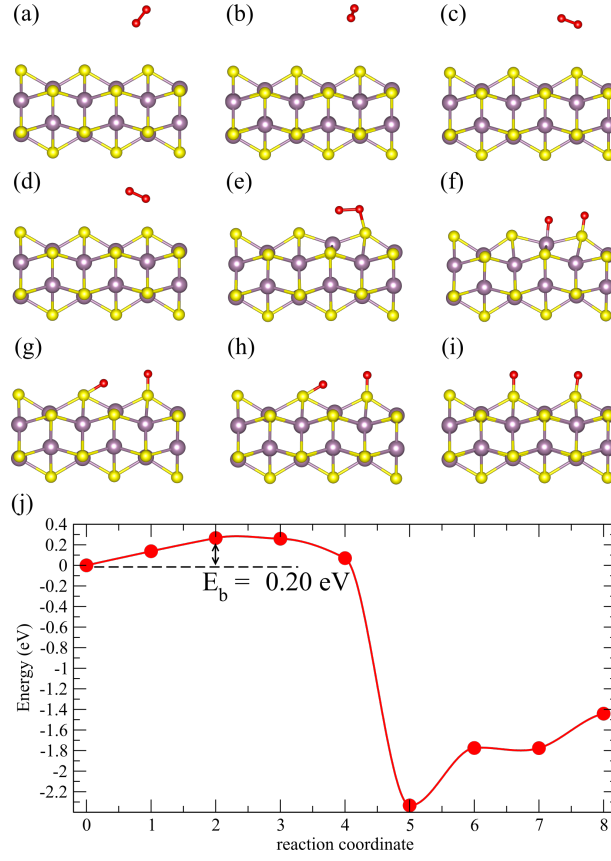


Figure 9: Minimum-energy reaction path for molecular oxygen on MoS nanowire at bridge position at $1/12$ ML coverage.

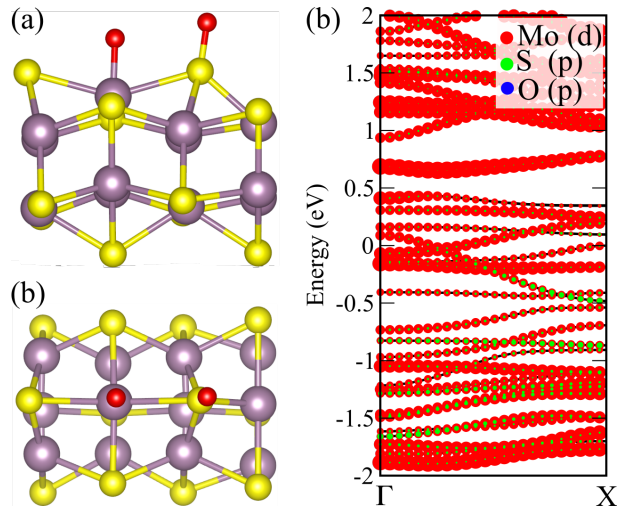


Figure 10: Electronic band structure and PDOS of the most stable configuration shown in Fig. 9.

program FOR1616. The calculations have been performed using the computational facilities of Supercomputer Santos Dumont at LNCC, QM3 cluster at the Bremen Center for Computational Materials Science CENAPAD-SP at Unicamp and LaMCAD at UFG.

References

- (1) Chhowalla, M.; Shin, H. S.; Eda, G.; Li, L.-J.; Loh, K. P.; Zhang, H. The chemistry of two-dimensional layered transition metal dichalcogenide nanosheets. *Nature Chem.* **2013**, *5*, 263–275.
- (2) Wang, Q. H.; Kalantar-Zadeh, K.; Kis, A.; Coleman, J. N.; Strano, M. S. Electronics and optoelectronics of two-dimensional transition metal dichalcogenides. *Nature Nanotechnol.* **2012**, *7*, 699–712.
- (3) Choi, W.; Choudhary, N.; Han, G. H.; Park, J.; Akinwande, D.; Lee, Y. H. Recent development of two-dimensional transition metal dichalcogenides and their applications. *Mater. Today* **2017**, 116.
- (4) Manzeli, S.; Ovchinnikov, D.; Pasquier, D.; Yazyev, O. V.; Kis, A. 2D transition metal dichalcogenides. *Nat. Rev. Mater.* **2017**, *2*, 17033.
- (5) Koverga, A. A.; Flórez, E.; J.-Orozco, C.; Rodriguez, J. A. Spot the difference: hydrogen adsorption and dissociation on unsupported platinum and platinum-coated transition metal carbides. *Phys. Chem. Chem. Phys.* **2021**, 20255–20267.
- (6) Chowdhury, T.; Sadler, E. C.; Kempa, T. J. Progress and Prospects in Transition-Metal Dichalcogenide Research Beyond 2D. *Chem. Rev.* **2020**, *120*, 12563–12591.
- (7) Lin, J. et al. Metallic Nanowires with Self-Adaptive Contacts to Semiconducting Transition-Metal Dichalcogenide Monolayers. *Nat. Nanotechnol.* **2014**, *9*, 436–442.

- (8) Liu, X.; Xu, T.; Wu, X.; Zhang, Z.; Yu, J.; Qiu, H.; Hong, J.-H.; Jin, C.-H.; Li, J.-X.; Wang, X.-R.; Sun, L.-T.; Guo, W. Top-down fabrication of sub-nanometre semiconducting nanoribbons derived from molybdenum disulfide sheets. *Nature Comm.* **2013**, *4*, 1776.
- (9) Souza, D. F.; Rosa, A. L.; Venezuela, P.; Padilha, J. E.; Fazzio, A.; Pontes, R. B. Structural evolution and the role of native defects in subnanometer MoS nanowires. *Phys. Rev. B* **2019**, *100*, 235416.
- (10) Ying, P.; Zhang, J.; Zhou, J.; Liang, Q.; Zhong, Z. Mechanical behaviors of MoS nanowires under tension from molecular dynamics simulations. *Comp. Mat. Sci.* **2020**, *179*, 109691.
- (11) Jin, K.-H.; Liu, F. 1D Topological Phase in Transition-Metal Monochalcogenides Nanowires. *Nanoscale* **2020**, *12*, 14661–14667.
- (12) Niu, S.; Cai, J.; Wang, G. Two-dimensional MOS2 for hydrogen evolution reaction catalysis: The electronic structure regulation. *Nano Research* **2021**, *14*, 1985–2002.
- (13) Koh, E. W. K.; Chiu, C. H.; Lim, Y. K.; Zhang, Y.-W.; Pan, H. Hydrogen adsorption on and diffusion through MoS2 monolayer: First-principles study. *International Journal of Hydrogen Energy* **2012**, *37*, 14323.
- (14) B.Zhao.; L.L.Liu.; D.Cheng, G.; T.Li.; N.Qi.; Chen, Z. Q.; Tang, Z. Interaction of O₂ with monolayer MoS₂: Effect of doping and hydrogenation. *Materials and Design* **2017**, *113*, 1–8.
- (15) Wang, K.; Paulus, B. Toward a Comprehensive Understanding of Oxygen on MoS₂: From Reaction to Optical Properties. *J. Phys. Chem. C* **2021**, *125*, 19544–19550.
- (16) Hohenberg, P.; Kohn, W. Inhomogeneous Electron Gas. *Phys. Rev.* **1964**, *136*, B864–B871.

- (17) Kohn, W.; Sham, L. J. Self-Consistent Equations Including Exchange and Correlation Effects. *Phys. Rev.* **1965**, *140*, A1133–A1138.
- (18) Kresse, G.; Joubert, D. From ultrasoft pseudopotentials to the projector augmented-wave method. *Phys. Rev. B* **1999**, *59*, 1758–1775.
- (19) Perdew, J. P.; Burke, K.; Ernzerhof, M. Generalized Gradient Approximation Made Simple. *Phys. Rev. Lett.* **1996**, *77*, 3865–3868.
- (20) Henkelman, G.; Jónsson, H. Improved tangent estimate in the nudged elastic band method for finding minimum energy paths and saddle points. *J. Chem. Phys.* **2000**, *113*, 9978–9985.
- (21) Henkelman, G.; Jónsson, H. A climbing image nudged elastic band method for finding saddle points and minimum energy paths. *J. Chem. Phys.* **2000**, *113*, 9901–9904.
- (22) Kristinsdóttir, L.; Skúlason, E. A systematic DFT study of hydrogen diffusion on transition metal surfaces. *Surf. Sci.* **2012**, *606*, 1400–1404.